The Nucleus **51**, No. 1 (2014) 109-115

The Nucleus
A Quarterly Scientific Journal of Pakistan Atomic Energy Commission
NCLEAM, ISSN 0029-5698

ELECTROCATALYTIC ACTIVITY OF $LiNiPO_4$ AND THE COPPER DOPED ANALOGUES TOWARDS OXYGEN REDUCTION

*N. KAUSAR JANJUA, M. MUMTAZ, A. YAQUB, S. SABAHAT[1] and A. MUJTABA

Department of Chemistry, Quaid-i-Azam University, Islamabad, Pakistan

[1]Department of Physics, COMSATS Institute of Information Technology, Park Road, Islamabad, Pakistan

(Received December 17, 2013 and accepted in revised form March 05, 2014)

Olivine type single phase LiNi(1-x)CuxPO4 ($0 < x < 0.99$) samples were successfully synthesized by non-aqueous sol-gel method followed by microwave (MW) annealing.. The phase purity, lattice parameters and morphology was confirmed by FTIR, XRD and SEM studies. X-Ray diffraction patterns of both the parent LiNiPO4 (LNP) and doped analogues were similar. Vegard law signifies a linear relation between lattice parameter and dopant concentration. Resultant change (either expansion or shrinkage) in lattice parameters as a result of doping means that effective doping is done showed effective doping by following the Vegard's law. Both LNP and its doped analogues were found to be electrocatalysts towards oxygen reduction which is apparently due to nanosized particles as obtained via MW annealing.

Keywords: Lithium nickel phosphate, XRD, Microwave annealing, Cyclic voltammetry, Oxygen reduction

1. Introduction

Presently the energy economy is in constant threat due to a dependence on non-renewable fossil fuels. The cleaner and alternative energy resources include the use of fuel cells, where oxygen reduction at cathode is one of the major reactions playing role in the performance [1]. The cathode reaction within fuel cell is basically the oxygen reduction reaction that needs to be monitored with efficiency [2]. Electrocatalyst is needed to increase the reaction kinetics and avoid large over potentials. Most common electro-catalyst for such application is Pt where the cost is the main barrier for using Pt at commercial scale. Thus new materials need to be explored or exiting ones need the tailoring of the properties. In this regard, lithium metal phosphates ($LiMPO_4$, where M = Fe, Mn, Co and Ni) with an ordered olivine structure are attractive candidates to be used as potential electrocatalyst for the fuel cell [3-5].

The crystal structure of $LiMPO_4$ is made up of two types of polyhedra, distorted MO_6 octahedral units that are corner shared and cross linked with PO_4 tetrahedral oxo-anions, forming 3-D network with tunnels that are occupied by Li ions along the (010) and (001) directions. In this network nearly close packed oxygen atoms in hexagons can be found with Li and M ions that are located at the center of octahedral sites [6]. It is believed that the strong PO_4 units tend to reduce the covalency of the M-O bond, modifying a useful potential for the M^{2+}/M^{3+} couple and thus producing a useful potential for lithium extraction and reinsertion [7]. The characteristics of this crystal lattice suggest that creation of vacancies (via doping) in the Li positions will generate potential sites for ionic jumping, with expected enhancement of Li mobility. It is established that low levels of dopants are indeed soluble in the olivine lattice up to the extent of 3 mol % in bulk materials [8]. In this paper, an attempt was made to substitute cations of different ionic radius i.e., Ni^{2+} with Cu^{2+}.

Current research focuses on the synthesis via non aqueous sol gel method and structural characterization of $LiNiPO_4$ along with the low level Cu doped analogues by XRD, FTIR, and morphology of the samples was studied by SEM. This paper reports microwave assisted non-aqueous sol gel synthesis of $LiNiPO_4$ where the high temperature sintering is surpassed by cost and time effective microwave treatment of the dried gel. Further the electrocatalytic activity of the synthesized compounds toward oxygen reduction was studied using cyclic voltammetry to access their potentiality.

2 Experimental Details

Metal nitrates i.e. $LiNO_3$ (Sigma Aldrich), $Ni(NO_3)_2.9H_2O$ (Sigma Aldrich), $Cu(NO_3)_2.6H_2O$ (Sigma Aldrich), and H_3P0_4(Riedel-de-Haën) were dissolved in $(CH_2)_2(OH)_2$ (Riedel-de-Haën) at room temperature at 298 K. The mixture was homogenous due to continuous stirring result in sol consisting of all the precursors. The temperature of the sol was raised slowly to353 K. The evolution of brown fumes indicated the removal of nitrates with gel formation. The get was dense in the beginning later it was dried.

* Corresponding author : nkusarjanjua@yahoo.com

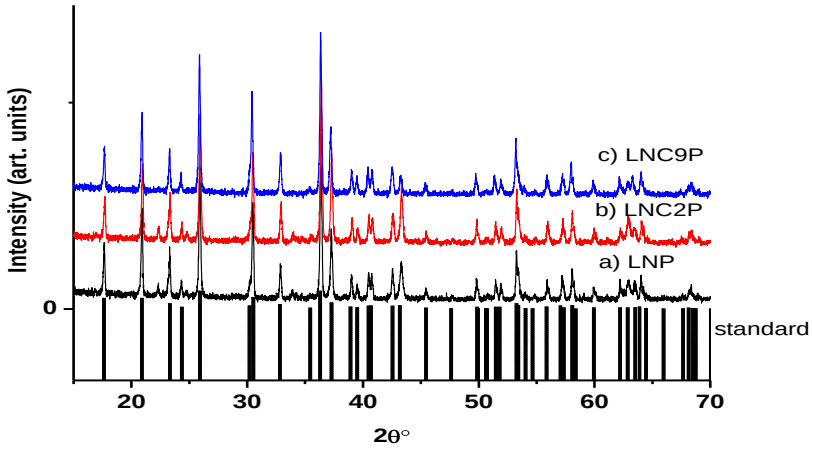

Figure 1. XRD patterns of $LiNi_{1-x}Cu_xPO_4$, a) x = 0.0, LNP b) x = 0.02, LNC2P and c) x = 0.09, LNC9P.

After evaporating the organics at about 573K for 2-3 hours the samples were exposed to the microwaves (model SGM 960, 2450 MHz, 220-240 V) for 20 minutes using a microwave oven. The final powders were analysed and applied for oxygen electro-catalysis.

2. Physical Characterization

X-ray diffraction technique on a Philips 1830 X-ray diffractometer (PW 3040/x0 X; Pert Pro) using Ni-filtered CuKα radiation ($K\alpha_1$= 1.5406Å) in the 2θ range 10–90° at a scan rate of $0.04^o s^{-1}$ was used for the phase formation of LNP and copper doped analogues. FTIR (Fourier transform infrared model BIO-RAD Excalibur FTS 3000/010-0221-2) technique was used to identify the functional groups. The crystalline olivine powder was mixed with KBr to form a pellet, and analysis was done in 400-2000 cm^{-1} region. The morphology of the samples was identified with SEM (Su 1500).

3. Electrochemical Studies

Cyclic voltammetric (CV) investigation was done to check the electrocatalytic properties of LNP and its Cu doped analogues for room temperature oxygen reduction. Three electrode assembly with glassy carbon electrode (GCE, 0.071 cm^2 area) as working, SCE as reference and Pt as counter electrodes was used for electrochemical measurement. The scans were taken in 50-900 mV s^{-1} range in 0.1 M KOH. To check the electrocatalytic effect of LNP, surface of glassy carbon was modified by dissolving 0.2 g powder in acetone and ethanol, sonicated for 5 min, and a small drop (4 µL) was casted onto the electrode, dried, and a drop of Nafion (4 µL) was added. The dried electrode is modified with all LNP materials and would be ready for use in cyclic voltammetric measurements.

3.1. Powder Diffraction Studies

Figure 1 of the synthesized powders shows single phase crystalline attained via microwave heating of LiNiPO4 and doped analogues, LiNi(1-x)CuxPO4 (x = 0.02 and 0.09) matching with reference code 00-032-0578. The crystal structure was indexed and refined by WinXPOW software with orthorhombic Pnma symmetry and exhibits well-formed crystallites with particle size in the range 35-62 nm. Figure 1 shows a well-resolved lattice indicating the crystallinity of the samples.

Normally the synthesis of LiNiPO4 requires strict controlling atmosphere, otherwise Ni3P exists [4] as an impurity. The impure structure is mainly segregated from the pristine compound by occurrence of a small impurity peak at 2θ value of 16.5° obtained in the reported solid state synthetic route for LNP [8]. This peak was not observed in the present synthesis showing pure phase formation via microwave assisted sol gel method. In this work using non aqueous sol gel method along with microwave heat treatment, single phase LiNiPO4 is obtained in air instead of inert atmosphere [9]. No additional peak was found for doped compositions, LiNi(1-x)CuxPO4 (x = 0.02 and 0.09) thus are single phased, as well (Figure 1b and 1c).

It is evident from figure 1 and cell parameters obtained by WinXPOW that Cu^{2+} doped powders crystallize in the Pnma crystal lattice. The $LiNi_{1-x}Cu_xPO_4$ X-ray diffraction patterns show resemblance with parent LNP. There exist a significant ionic radii difference between Cu^{2+} (87 pm), Ni^{2+} (83 pm) and Li^+ (90 pm) [10]. As a result of the added copper the coulombic interaction between the cations increase therefore volume of the cell is varied as depicted in Figure 2. Interestingly, the substitution of Cu^{2+} results an increase in cell parameters a and c while the lattice parameter b decreases with increase in dopant level. The linear relationship is in agreement with Vegard's law [11].

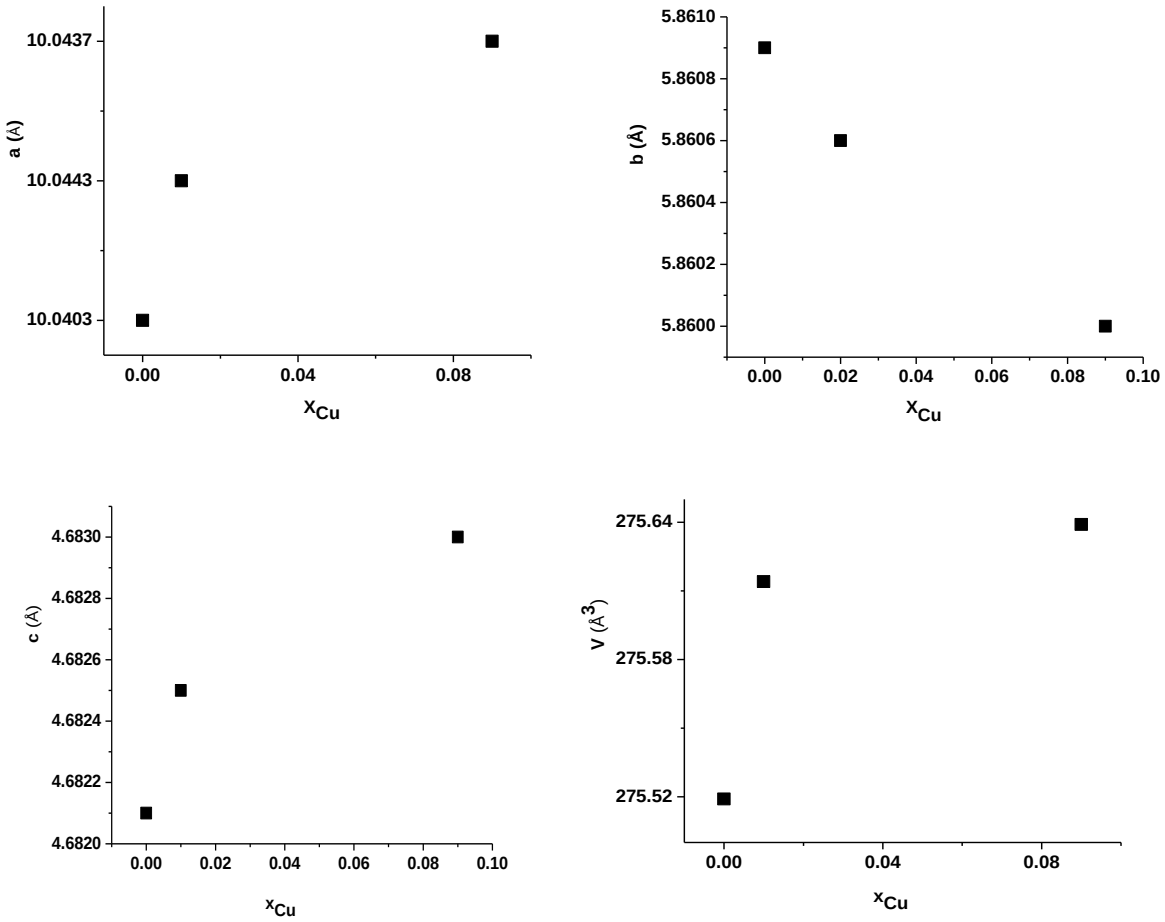

Figure 2. Dependence of cell parameters upon copper content in LiNi1-xCuxPO4 (x = 0.0, 0.02, and 0.09).

The dependence of cell parameters on Cu dopant level is graphically represented in figure 2 which shows that as Cu content increases, the cell parameters a and c increase while b decreases. There is net expansion of unit cell volume with Cu doping.

A small extent of f peak broadening is observed in X-ray patterns of the doped powders. The crystallite size was calculated using the peak broadening by Debye Scherrer equation, as under [11]:

$$D_{av} = \frac{k\lambda}{\beta \cos\theta} \quad (1)$$

Where k is the shape factor (0.9), λ is 0.154 nm, β is the FWHM and θ is the peak position [12-14]. The particle size is 35 nm for the pristine compound, whereas 59.97 nm and 62.03 nm, for LNC2P and LNC9P, respectively.

3.2. FTIR Study of Synthesized Powders

FTIR studies revealed the lattice dynamics and structural properties of the olivine samples in 4000-400 cm^{-1} frequency range. All the compounds exhibited similar spectra in good agreement with the structural results. The IR features two fundamental vibrations above 400 cm^{-1} i.e. ν_2 and ν_4 of PO_4^{3-}group in an olivine structure. The spectrum involves mainly O-P-O symmetric and antisymmetric bending modes with a small contribution of P vibration, such as ν_2 and ν_4 in the regions 400-470 cm^{-1} and 575- 665 cm^{-1}, respectively [15-17]. In case of LNP the high frequency band of FTIR absorption spectra at 650 cm^{-1} and 663 cm^{-1} is attributed to the stretching mode of NiO_6 distorted octahedral. NiO_6 octahedra undergo a degree of distortion due to the new incoming cation. The structural distortion is mainly depicted by the appearance of new broad bands at 1510 cm^{-1} and 1263 cm^{-1} [18,19]. The changes are due to the vibrational and stretching modes. Figure 3 is evidenced for this observation.

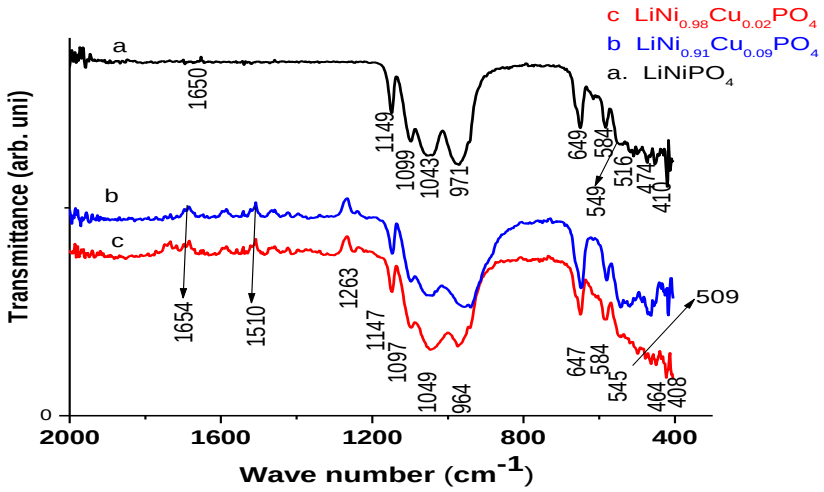

Figure 3. FTIR spectra of pure $LiNiPO_4$ alongwith the doped analogues (LNC_2P and LNC_9P).

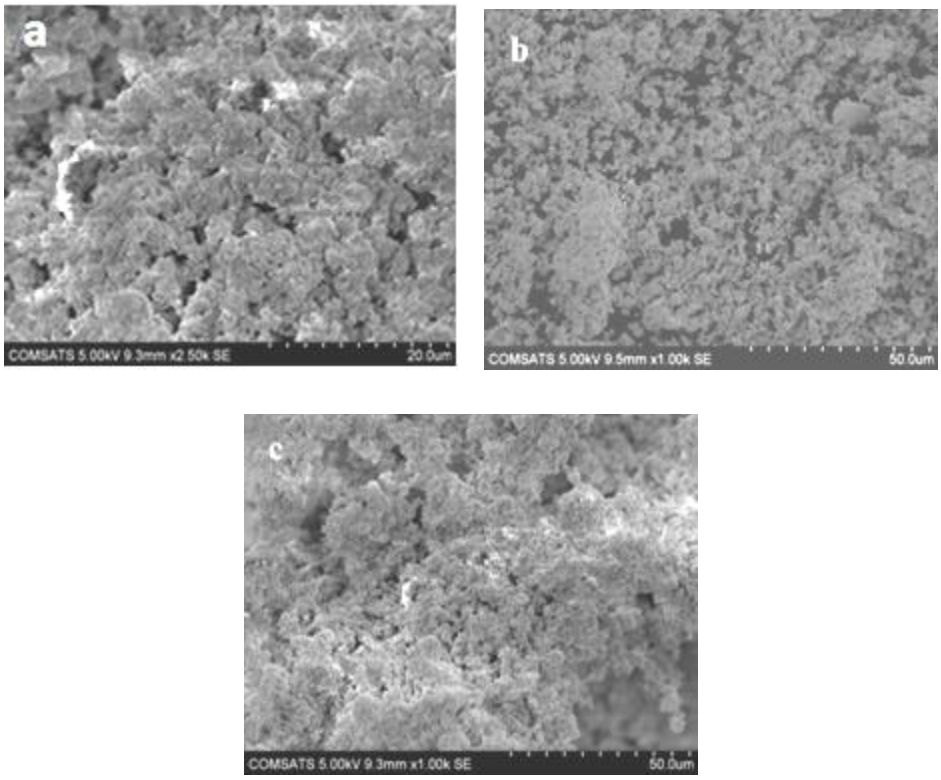

Figure 4. (a) Scanning electron micrographs of LNP, (b) its Cu doped analogues $LiNiC_2P$ and (c) $LiNiCu_9P$.

3.3. Scanning Electron Studies

The SEM images in Figure 4 (a, b and c) corresponded to homogeneously distributed particle size. Apparently, particles are quite similar and small in size for all the synthesized compounds. However, some are gathered to form protuberances as LNP shows aggregates of ~10µm. [X-ray diffraction patterns revealed the true variation in their sizes]. Present low temperature synthesis treatment helps to get smaller particles. In addition, homogeneous sizes result in enhanced electrocatalytic activity as later observed in electrochemical oxygen reduction process. The electrode modification is required which needs homogeneity in particle size for favorable application of $LiNiPO_4$ as cathode material for battery applications. The Cu doped analogues also showed the similar microscopic structures.

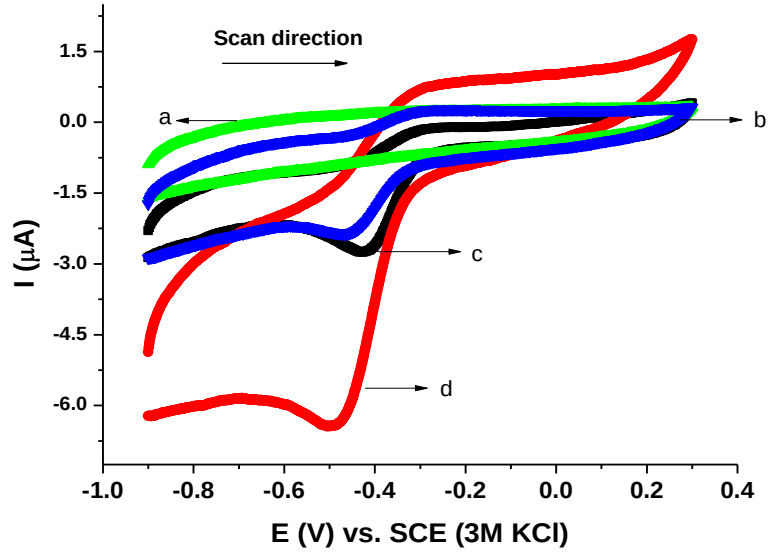

Figure 5. Cyclic voltammograms for uncoated glassy carbon in (a) absence of oxygen, (b) presence of oxygen and LNP, (c) $LiNiCu_9P$ coated glassy carbon electrode and (d) in presence of oxygen in alkaline medium.

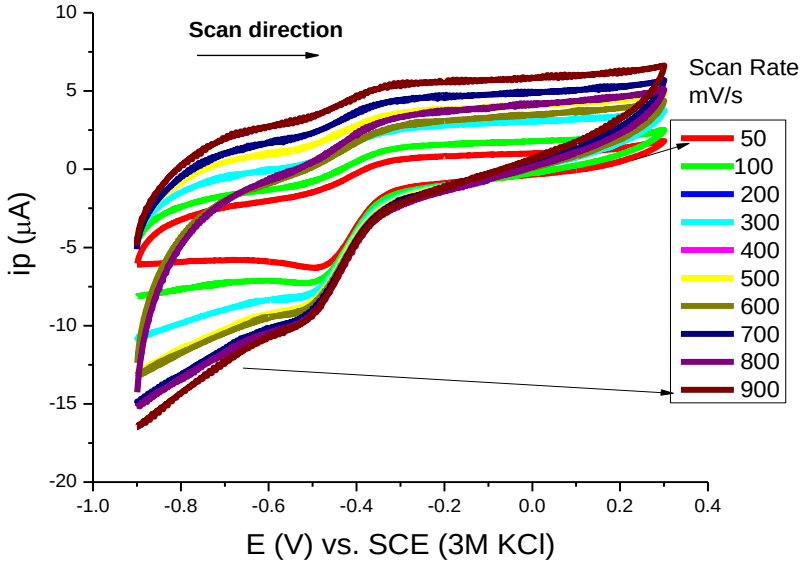

Figure 6. Effect of scan rate on the peak current for $LiNiCu_9P$ coated glassy carbon electrode in presence of oxygen in alkaline medium.

3.4. Electrocatalytic Testing

To evaluate the electrocatalytic performance of LNP and its Cu doped analogues towards oxygen reduction, cyclic voltammetry was done on bare as well as coated glassy carbon electrode in an alkaline medium consisting of 0.1 M KOH. The resulting voltammograms are displayed in figure 5. It can be seen that in the peak current corresponding to oxygen reduction reaction increase considerably after coating glassy carbon electrode with LNP mentioned samples labels in each sentence. Even Cu doping further improves the current. It can be seen that in absence of oxygen, no or diminished peak was observed in each case of bare and modified GCE. Figure 5d gives the obvious electrocatalytic activity of $LiNiCu_9P$ coated GCE for oxygen reduction reaction. Thus it can be inferred that the pronounced peak in cathodic scan is due the oxygen reduction which is not very clear at bare GCE. Similarly, cyclic voltammograms were obtained after multi scans which demonstrated good chemical and electrochemical stability of LNP and its Cu doped analogue towards oxygen reduction reaction at glassy carbon electrode. On scanning towards negative potential window, a single peak was observed which could be attributed to electrochemical reduction of oxygen (Figure 6).

Table 1. Derived electrochemical parameters using electrochemical data

Samples	i_p (μA)	Ep (V)	Ep/2 (V)	(Ep-Ep/2) (V)	αn
$LiNiCu_9P$	6.45	-0.461	-0.350	0.111	0.43
LNP	2.78	-0.426	-0.341	0.085	0.56

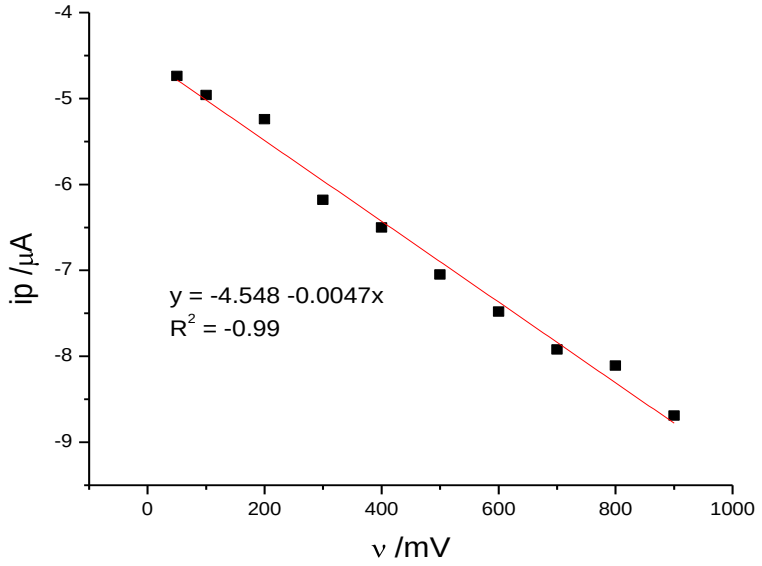

Figure 7. Linear relationship between peak currents with the scan rate for $LiNiCu_9P$ coated glassy carbon electrode in presence of oxygen in alkaline medium.

The value of αn was calculated using the equation [20]:

$$\alpha n = \frac{47.7}{Ep - E_{p/2}} mV \qquad (2)$$

These values are tabulated in Table 1 and correspond to a one electron reduction of oxygen. Various possible electrochemical parameters as obtained from CV data depict that these materials facilitate the electron transfer process to electro reduce oxygen. Also, the quasi-reversible nature of electrochemical reduction of oxygen in basic media can be accessed from Ep-Ep/2 values [21, 22] (Table 1). These trends are supported by the linear relationship between peak currents with the scan rate as depicted by Figure 7.

4. Conclusions

Non aqueous sol gel method proved successful to synthesize LNP and copper doped analogues. Microwave annealing is energy, cost and time effective, compared to the conventional furnace heating process. The crystallite size calculated by using Scherrer's eq. is in nm range. The X-ray studies confirm the phase pure crystalline compositions with nano sized particles which are also in accordance with the SEM results. The FTIR studies show the particular vibrational and stretching modes for the crystal lattice of these materials. The synthesized compounds showed promising electrocatalytic activity towards oxygen reduction reaction making these as potential electrocatalysts. It is anticipated that adopted low-energy and low-cost synthetic route is suitable for viable synthesis of catalytic materials for such important reactions like oxygen reduction reaction.

Acknowledgements

The authors are thankful to the Quaid-i-Azam University, Islamabad for URF grant.

References

[1] L. Carrette, K.A. Friendrich and U. Stimming, Fuel Cells-Fundamentals and Applications **1** (2001) 5.

[2] K. Kinoshita, Electrochemical Oxygen Technology (John Wiley & Sons 1992).

[3] H. Li, G. Azuma and M. Tohda, Electrochem. Solid State Lett. **5** (2002) A135.

[4] P.S. Herle, B. Ellis, N. Coombs and N.F. Nazar, Nat. Matter. Lett. **3** (2004) 147.

[5] J. Wolfenstine and J. Allen, J. Power Sources, **136** (2004) 150.

[6] I. Abrahams and K.S. Easson, Acta Crystallogr. C, **49** (1993) 925.

[7] M.C. Tucker, M.M. Doeff, T.J. Richardson, R. Finones, E.J. Cairns and J.A. Reimer, J. Am. Chem. Soc. **5** (2002) A95.

[8] M. Wagemaker, B.L. Ellis, D.L. Hecht, F.M. Mulder and L.F. Nazar, Chem. Mater. **20** (2008) 6313.

[9] M. Minakshi, P. Singh, D. Appadoo and D.E. Martin, Electrochim. Acta, **56** (2011) 4356.

[10] L.E. Smart and E.A. Moore, Solid State Chemistry: An Introduction, 3rd Ed. (Taylor & Francis 2005).

[11] A. Goni, L. Lezama, M.I. Arriortua, G.E. Barberis and T. Rojo, J. Mater. Chem. **10** (2000) 423.

[12] A.R. West, Solid State Chemistry and its Application. Student Ed. (Wiley and Sons 1998).

[13] B.D. Culity, Elements of X-Ray Diffraction, 2nd Ed. Addison Wesley Pub. Co., Reading (1978).

[14] C. Suryanarayana and M.G. Norton, X-Ray Diffraction: A Practical Approach, 1st Ed. (Springer Business Media, New York (1998).

[15] C. Julien, M.A. Camacho-Lopez, T. Mohan, S. Chitra, P. Kalyani and S. Gopukumar, Solid State Ionics, **135** (2000) 241.

[16] M.T. Paques-Ledent and P. Tarte, Spectrochim. Acta **30** (1974) A:673.

[17] A. Rulmont, R. Cahay M. Liegevis and P. Tarte, Eur. J. Sol. State Inorg. **28** (1991) 207.

[18] K. Nakamoto, Infrared and Raman Spectra of Inorganic and Coordination Compounds.4th Ed., Wiley and Sons (1978).

[19] V. Ramar, K. Saravanan, S.R. Gajjela, S. Hariharan and P. Balaya, Electrochim. Acta, **105** (2013) 496.

[20] A.J. Bard and L.R. Faulkner, Electrochemical Methods: Fundamentals and Applications, John Wiley (1980).

[21] Y. Wang, D. Zhang and H. Liu, J. Power Sources **195** (2010) 3135.

[22] K. Arihara, L. Mao, P.A. Liddell, E. Marino-Ochoa, A.L. Moore, T. Imase, D. Zhang, T. Sotomura and T. Ohsaka, J. Electrochem. Soc. **151** (2004) A 2047.